Role of the cytosolic loop C2 and the C-terminus of YidC in ribosome binding and insertion activity

Geng, Yanping; Kedrov, Alexej; Caumanns, Joseph J; Crevenna, Alvaro H; Lamb, Don C; Beckmann, Roland; Driessen, Arnold J M

Published in:
The Journal of Biological Chemistry

DOI:
10.1074/jbc.M115.650309

Publication date:
2015

THE JOURNAL OF BIOLOGICAL CHEMISTRY VOL. 290, NO. 28, pp. 17250–17261, July 10, 2015

Role of the Cytosolic Loop C2 and the C Terminus of YidC in Ribosome Binding and Insertion Activity*

Received for publication, March 9, 2015, and in revised form, May 12, 2015 Published, JBC Papers in Press, May 28, 2015, DOI 10.1074/jbc.M115.650309

Yanping Geng[‡], Alexej Kedrov[§], Joseph J. Caumanns[‡], Alvaro H. Crevenna[¶], Don C. Lamb[¶], Roland Beckmann[§], and Arnold J. M. Driessen[‡1]

From the [‡]Molecular Microbiology, Groningen Biomolecular Sciences and Biotechnology Institute and Zernike Institute for Advanced Materials, Nijenborgh 7, 9747 AG Groningen, The Netherlands, the [§]Gene Center Munich and the [¶]Physical Chemistry, Department for Chemistry, Center for Nanoscience, the NanoSystems Initiative Munich and the Center for Integrated Protein Science Munich, Ludwig-Maximilians-University, 81377 Munich, Germany

Background: The C terminus of YidC is not the sole determinant for ribosome binding.
Results: The cytosolic loop C2 of YidC is involved in ribosome binding and membrane insertion.
Conclusion: The cytosolic loop C2 and the C terminus of YidC are crucial for maintaining a functional YidC·ribosome complex during membrane insertion.
Significance: Understanding the structural basis of the YidC·ribosome interaction provides insights in the YidC insertion mechanism.

Members of the YidC/Oxa1/Alb3 protein family mediate membrane protein insertion, and this process is initiated by the assembly of YidC·ribosome nascent chain complexes at the inner leaflet of the lipid bilayer. The positively charged C terminus of *Escherichia coli* YidC plays a significant role in ribosome binding but is not the sole determinant because deletion does not completely abrogate ribosome binding. The positively charged cytosolic loops C1 and C2 of YidC may provide additional docking sites. We performed systematic sequential deletions within these cytosolic domains and studied their effect on the YidC insertase activity and interaction with translation-stalled (programmed) ribosome. Deletions within loop C1 strongly affected the activity of YidC *in vivo* but did not influence ribosome binding or substrate insertion, whereas loop C2 appeared to be involved in ribosome binding. Combining the latter deletion with the removal of the C terminus of YidC abolished YidC-mediated insertion. We propose that these two regions play an crucial role in the formation and stabilization of an active YidC·ribosome nascent chain complex, allowing for co-translational membrane insertion, whereas loop C1 may be involved in the downstream chaperone activity of YidC or in other protein-protein interactions.

In eubacteria, membrane proteins constitute ~30% of the total proteins synthesized in the cell (1). They participate in signal transduction, respiration, energy generation, as well as the transport of a variety of ions, solutes, and macromolecules. The majority of the inner membrane proteins are destined for and inserted into the membrane via the SecYEG translocon-mediated pathway (2, 3). However, a specific subset of membrane proteins requires YidC insertase for integration into the membrane. *Escherichia coli* YidC is an abundant membrane protein, with ~2500 copies per cell (1) and it is involved in the insertion, folding and/or assembly of membrane proteins into the cytoplasmic membrane independently or in concert with the SecYEG translocon (4). *E. coli* YidC is essential for cell viability (5) and has been shown to function as an insertase in the membrane insertion of the filamentous phage Pf3 coat and M13 pro-coat proteins (5, 6) and the endogenous substrates F_0c (7), MscL (8, 9), and TssL (10). In cooperation with the Sec translocase, YidC assists in the membrane insertion of CyoA (11, 12), NuoK (13), and F_0a and F_0b subunits of F_1F_0 ATPase (14), and the translocation of the periplasmic loop 1 and loop 2 of TatC (15). It also acts as a chaperone in the folding of lactose permease LacY and MalF (16, 17).

All members of the YidC/Oxa1/Alb3 protein family share a very conserved hydrophobic core region consisting of five transmembrane segments (TMS)[2] connected by hydrophilic loops (18), but the *E. coli* YidC possesses an extra N-terminal TMS1 linked by a large periplasmic domain P1 to the TMS2 (19). Recently, Kumazaki *et al.* (20) reported the crystal structures of YidC2 from *Bacillus halodurans* and YidC of *E. coli*, both solved in the lipid environment. The high resolution structures revealed that the global arrangements of the conserved core regions in *E. coli* YidC and *B. halodurans* YidC2 are in high

* This work was supported by Chemical Sciences and Earth and Life Sciences that are both subsidized by the Netherlands Foundation for Scientific Research and by the Chinese Scholarship Council. This work was also supported by a European Research Council Advanced Grant (to R. B.), Deutsche Forschungsgemeinschaft Grant SFB 646 B11 (to D. C. L.), and funds from the Excellent Clusters Nanosystems Initative Munich, the Center for Integrated Protein Science Munich, the Ludwig-Maximilians-Universität München via the LMUInnovativ BioImaging Network, and the Center for NanoScience (to D. C. L.).

[1] To whom correspondence should be addressed: Molecular Microbiology, Groningen Biomolecular Sciences and Biotechnology Inst. and Zernike Inst. for Advanced Materials, Nijenborgh 7, 9747 AG Groningen, The Netherlands. Tel.: 31-50-3632164; Fax: 31-50-3632154; E-mail: a.j.m.driessen@rug.nl.

[2] The abbreviations used are: TMS, transmembrane segment; RNC, ribosome nascent chain; DDM, *n*-dodecyl β-D-maltoside; MSP, major scaffold protein; Nd, nanodisc; mono, monomeric form; IPTG, isopropyl 1-thio-β-D-galactopyranoside; FCS, fluorescence correlation spectroscopy; NTA, nitrilotriacetic acid; Tricine, *N*-[2-hydroxy-1,1-bis(hydroxymethyl)ethyl]glycine.

TABLE 1
Strains and plasmids used in the study

Plasmid/strain	Description	Source
Plasmids		
pTrc99a	Expression vector	
pKA107	YidC(C423S, D269C)	Ref. 24
pKA120	YidC(C423S, D269C) Δ374–383; YidCΔ1	This study
pKA121	YidC(C423S, D269C) Δ385–394; YidCΔ2	This study
pKA122	YidC(C423S, D269C) Δ392–401; YidCΔ3	This study
pKA123	YidC(C423S, D269C) Δ401–410; YidCΔ4	This study
pKA124	YidC(C423S, D269C) Δ410–419; YidCΔ5	This study
pKA125	YidC(C423S, D269C) Δ485–489; YidCΔ6	This study
pKA126	YidC(C423S, D269C) Δ489–493; YidCΔ7	This study
pKA131	YidC(C423S, D269C) Δ536–547; YidCΔC	Ref. 24
pYP00	YidC(C423S, D269C) Δ485–489,Δ536–547; YidCΔ8	This study
pETNuoK	pET20 containing *nuoK* gene	Ref. 13
pET20MscL	MscL	Ref. 9
pET2302	SecYEG	Ref. 38
pJK763	RNC-F_0c44 SecM-stalled	Ref. 24
pEM36-F_0c	RNC-F_0c TnaC-stalled	Ref. 27
***E. coli* strains**		
DH5α	*supE44 hsdR14 recA1 endA1 gyrA96 thi-1 relA1ΔlacU169* (Φ80*lacZ* ΔM15); K12 derivative	Ref. 39
FTL10	*FTL10 yidC attB:: (araC$^+$ P_{BAD} yidC$^+$); Kan^r*	Ref. 28
SF100	*F-, ΔlacX7, galE, galK, thi, rpsL, strA 4, ΔphoA(pvuII), ΔompT*	Ref. 29

agreement with the folding of the five TMSs into a positively charged groove, whereas the hairpin-like C1 domain that consists of two antiparallel helices is more flexible in the *E. coli* YidC.

Like the SecYEG translocon, the YidC protein family facilitates co-translational substrate insertion involving ribosome binding to initiate the insertion process. The C-terminal regions of the mitochondrial Oxa1 and *Streptococcus mutants* YidC1 and YidC2 have been shown to be crucial for the contact with ribosomes (21–23), and deletions within these domains compromised the protein insertion function. In *E. coli*, the C terminus of YidC is positively charged, but it is substantially shorter (13 residues; total charge +5) in comparison with Oxa1 (86 residues; +14), YidC1 (33 residues; +9), and YidC2 (61 residues; +14) (19, 22, 23). Recently, we have investigated the interaction of YidC with translation-stalled ribosomes by means of the fluorescence correlation spectroscopy (FCS) technique under physiological condition using nanodisc-embedded YidC to mimic the native lipids environment (24). In contrast to earlier models (25), we found that monomeric *E. coli* YidC was sufficient for ribosome binding, and thus it formed a minimal functional unit. The analysis highlighted the role of the C terminus of YidC in the ribosome binding but also suggested it to be not the sole determinant, so alternative ribosomal contacting sites were proposed within the positively charged C1 and C2 domains of YidC (25). The chimeric *E. coli* YidC with an extended C-terminal tail from *Rhodopirellula baltica* YidC (YidC-Rb) exhibited enhanced binding of translating ribosome forming primary interaction sites on the ribosomal rRNA helix 59 and the ribosomal protein L24, as shown by the cryo-electron microscopy structure of the YidC-Rb·RNC complex (26). Lately, Wickles *et al.* (27) built a structural model of *E. coli* YidC via the intramolecular co-variation analysis, which appeared in agreement with the experimentally solved structure. The model was applied to interpret the interaction of *E. coli* YidC with the RNC-F_0c visualized in cryo-electron microscopy. The residues Tyr-370 and Tyr-377 in the C1 loop and Asp-488 in the C2 loop of YidC were suggested to be directly engaged in the ribosome binding at His-59 and the protein Leu-23, respectively (27). Substitution of the residues compromised the vegetative growth of cells; however, the role of cytoplasmic loops in ribosome binding and insertion activity of YidC has not been studied.

Here, we aimed to determine the regions of YidC involved in ribosome binding and further investigate the contribution of the YidC·ribosome physical interaction to the insertion process. Herein, we made sequential deletions within the C1 and C2 loops of *E. coli* YidC and studied their activity *in vitro* by means of biochemical and biophysical assays and also checked functional properties of these YidC variants *in vivo*. Truncations within loop C2 reduced ribosome binding to YidC at the membrane interface and combining deletions within C2 and at the C terminus of YidC also inactivated YidC in membrane insertion of F_0c and MscL, suggesting that these two sites build a platform for ribosome docking. On the other hand, modifications within the loop C1 severely affected *in vivo* functioning of YidC but did not interfere with ribosome binding or substrate insertion, suggesting that the C1 loop is involved in chaperone/foldase activity of YidC or protein-protein interactions at the membrane interface or the insertion of yet unknown YidC substrates that are essential for cell viability.

Experimental Procedures

Bacterial Strains and Plasmids—The YidC depletion strain *E. coli* FTL10 (28) was a kind gift of Frank Sargent (University of East Anglia, Norwich, UK). *E. coli* SF100 (29) was used to express the YidC variants. Plasmid pKA107 was used as the template, in which the endogenous cysteine residue at position 423 of YidC was substituted for a serine, whereas a solvent-exposed cysteine was introduced at position 269, which did not affect the functionality (24). Primers were designed annealing to the flanking regions of the selected deletions in the cytosolic loops C1 and C2 of *E. coli* YidC (Table 1). PCR products containing truncated *yidC* genes were treated with DpnI at 37 °C for 2 h and then subject to gel purification. After phosphorylation and self-circularization, the resulting plasmids were multiplied in DH5α cells and verified by DNA sequencing. Plasmids containing the genes encoding for YidC mutated proteins were

subject to Eco88I (AvaI) and HindIII double digestion, and the obtained DNA fragments with truncated *yidC* genes were recloned into fresh pTrc99a, yielding plasmids pKA120–126 (Table 1). As for the mutated *yidC* gene containing deletions in the C2 domain and at the whole C terminus, PCR was carried out using plasmid pKA125 as the template. The resulting *yidC* double truncated gene was subject to XbaI and HindIII double digestion and cloned into XbaI/HindIII double-digested pTrc99a vector, yielding the construct pYP00.

In Vivo Complementation Assay—To study the functionality of *E. coli* YidC variants, *E. coli* FTL10 cells were transformed with plasmids harboring genes encoding for mutated YidC proteins and grown under aerobic or anaerobic conditions. For aerobic growth, cells were grown overnight in the LB medium supplemented with 0.2% arabinose (w/v) and ampicillin (100 μg/ml). To deplete YidC, overnight cultures were diluted into fresh LB medium supplemented with 0.2% glucose (w/v) and ampicillin (100 μg/ml) and grown at 37 °C for 3 h. After adjusting to the same A_{600}, 10-fold dilution series of each culture were made and 3 μl of each dilution was spotted on LB plates in the presence of 0.2% arabinose (w/v) or 0.2% glucose (w/v) and 50 μM isopropyl 1-thio-β-D-galactopyranoside (IPTG). The plates were incubated at 37 °C at least 10 h, and the growth phenotype of the diluted cultures displayed on LB plates supplemented with glucose and IPTG represents the deletion effect on YidC function. For the anaerobic growth, cells were grown overnight at 37 °C in the basal anaerobic medium containing K_2HPO_4 (0.7%), KH_2PO_4 (0.2%), NH_4Cl (0.1%), $MgSO_4{\cdot}7H_2O$ (0.02%), $CaCl_2{\cdot}2H_2O$ (0.002%), SL9 trace element solutions (0.1% v/v) supplemented with the carbon source glycerol (0.5% v/v) and the electron acceptor sodium fumarate (10 mM), and 0.2% arabinose (w/v) was supplied initially to induce the expression of endogenous *yidC* gene. To deplete the endogenously expressed YidC, overnight cultures were collected and washed twice with basal anaerobic medium and were diluted 2-fold into the same medium supplemented with glycerol and sodium fumarate. The procedure was repeated until the growth cessation. The cells were subsequently serially diluted, and 3 μl of the cell suspension were spotted on anaerobic medium plates containing 0.2% arabinose (w/v) or 50 μM IPTG and 0.5% glucose, respectively. The anaerobic growth was carried out in sealed bottles under O_2-free environment.

Protein Purification and YidC Labeling—Histidine-tagged YidC proteins or SecYEG were expressed into *E. coli* SF100, and the inner membrane vesicles were prepared as described previously (24, 30). Target proteins were purified by Ni^+-NTA affinity chromatography. Firstly, inner membrane vesicles were solubilized in 50 mM Tris-HCl, pH 8.0, 1% *n*-dodecyl β-D-maltoside (DDM), 100 mM KCl, and 10% glycerol at 4 °C for 30 min. As for YidC variants, 200 μM tris (2-carboxyethyl) phosphine was added to inhibit disulfide bonds formation. Then solubilized proteins were mixed with Ni^+-NTA-agarose beads for 1 h at 4 °C on a rolling bank, washed with 3 bed volumes of buffer A (50 mM Tris-HCl pH 8.0, 0.1% DDM, 100 mM KCl, 10% glycerol) supplemented with 50 mM imidazole, and finally eluted with 300 mM imidazole in buffer A. For optional labeling, Ni^+-NTA-bound YidC variants were incubated with the labeling buffer B (100 mM K_2HPO_4/KH_2PO_4, pH 7.0, 0.1% DDM, 100 mM KCl, 10% glycerol, and 200 μM tris (2-carboxyethyl) phosphine) supplemented with 200 μM Alexa Fluor 488 C_5-maleimide (Life Technologies/Invitrogen) for 2 h at 4 °C on a rolling bank, followed by extensive washing with 10 mM imidazole and finally eluted by 400 mM imidazole in buffer B. Protein concentration and labeling efficiency were estimated spectrophotometrically. The extinction coefficient values for YidC at 280 nm and Alexa Fluor 488 at 500 nm were 96,000 and 72,000 cm^{-1} M^{-1}, respectively.

Nanodisc Reconstitution of YidC—To ensure a native membrane environment, the fluorescently labeled YidC variants were reconstituted into the lipid bilayers supported by the major scaffold protein (MSP) to form nanodiscs according to the previous method with minor modifications (24, 31) Synthetic membranes composed of DOPG:DOPE:DOPC (dioleoylphosphatidylglycerol: dioleoylphosphatidylethanolamine:dioleoylphosphatidylcholine) at a molar ratio of 3:3:4 were used to generate stable nanodiscs (32). To obtain nanodiscs containing single YidC molecule ($YidC^{mono}$-Nd), detergent-destabilized lipids were mixed with MSP1D1 and YidC at the molar ration of 250:10:1. The YidC-containing nanodiscs were spontaneously assembled upon removal of the detergent by Bio-Beads SM2 sorbent (Bio-Rad), yielding nanodiscs with a diameter of ~10 nm (33). Size exclusion chromatography was then employed to separate the empty nanodiscs and $YidC^{mono}$-Nd. YidC-enriched factions were used for FCS measurement. For preparing empty nanodiscs, 2% of fluorophore-conjugated DOPE-Atto 488 (Atto Tech) was added to the lipid formulation, and lipids and MSP were mixed at the molar ratio 25:1.

Ribosome Nascent Chain Isolation—Generation of SecM-stalled ribosomes carrying the F_0c nascent polypeptide chain was performed as described (24, 34). The stalled polypeptide chain is composed of N-terminal 3× Strep tag followed by a sequence encoding for the 1–44 residues of F_0c containing the first TMS and flanking polar regions, with SecM arresting sequence fused to the C terminus. RNCs were expressed *in vivo* in *E. coli* and isolated by a StrepTactin affinity chromatography (IBA) as previously described (34). TnaC-stalled RNCs were prepared *in vivo* according to the published protocol (35). The N-terminal polyhistidine tag at the F_0c nascent chain was removed upon specific proteolysis by the 3C protease.

Fluorescence Correlation Spectroscopy—FCS experiments were performed on the inverted confocal microscopy LSM710 in combination with the Confocor 3 module (Zeiss GmbH) and on a home-built set-up described previously (36). Prior to the experiment, the known diffusion coefficient of Alexa Fluor 488 in water was used to calibrate the confocal volume (D = 400 $\mu m^2/s$) (37). To analyze the interactions between fluorescently labeled YidC and RNC-F_0c, $YidC^{mono}$-Nd was diluted to a final concentration of ~50 nM in buffer (50 mM HEPES-KOH, pH 7.2, 100 mM KCl, 5% (v/v) glycerol, and 5 mM $MgCl_2$), and a 5-fold excess of RNCs was added. The reaction was incubated at room temperature for 5–10 min before subject to the FCS measurement. The fluctuation of fluorescence arising from the fluorescent YidC-Nd complexes was monitored and autocorrelated over the time to measure average diffusion time. Autocorrelation curves were fitted using the two-component model as described in the previous study (24, 34). The individual diffu-

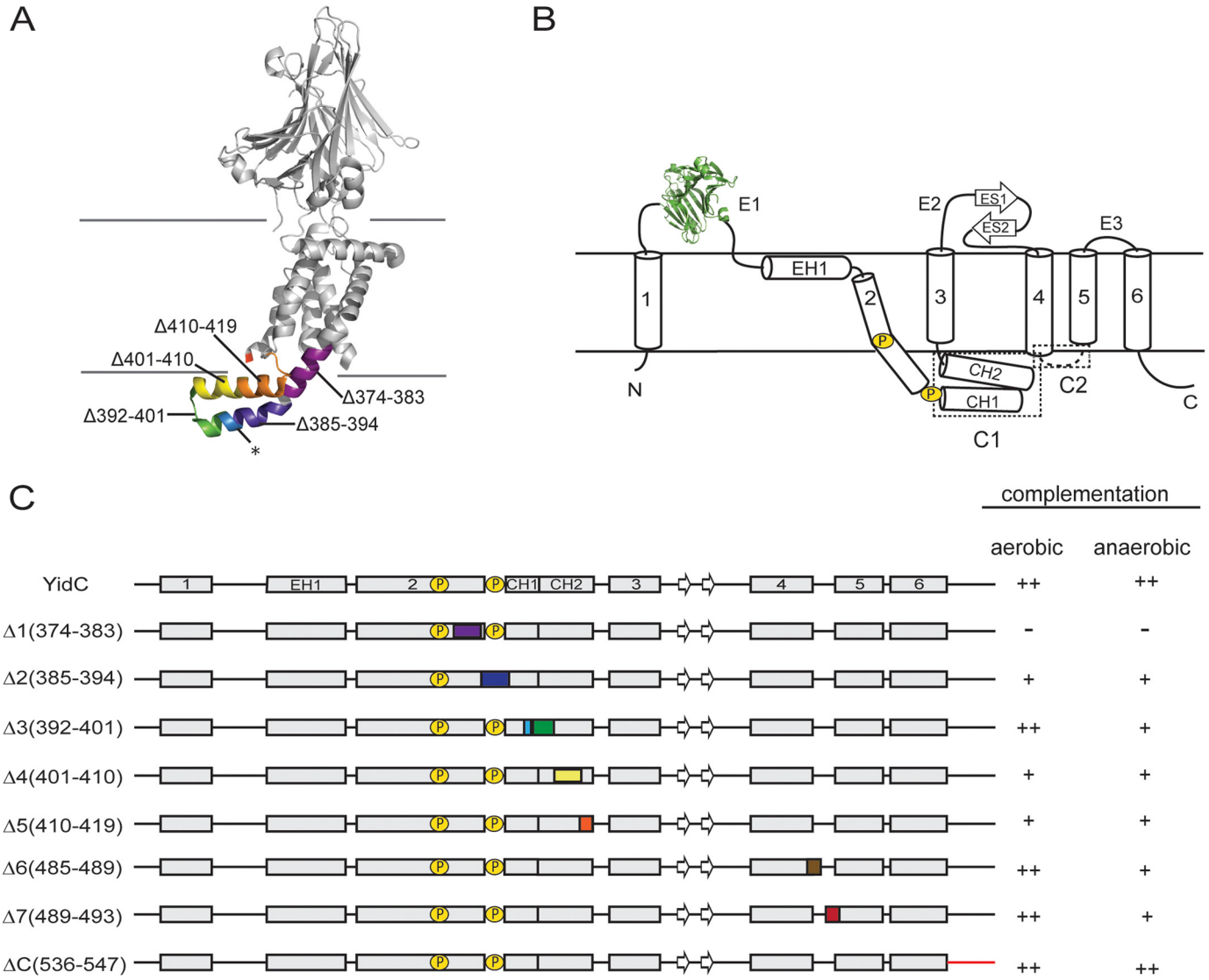

FIGURE 1. **Overview of *E. coli* YidC variants.** *A*, a ribbon representation of the *E. coli* YidC structure. The short regions of *E. coli* YidC that were deleted are colored in the range of *purple* to *red* from the N terminus to the C terminus. The cytosolic loop C2 and the C terminus are structurally disordered. *B*, a topology diagram of *E. coli* YidC. Helices and strands are indicated by *cylinders* and *arrows*, respectively. The CH1 and CH2 helices in the cytosolic loop C1 fold into a hairpin-like structure. The cytoplasmic loops C1 and C2 are highlighted in the *dashed boxes*. *C*, a schematic representation of designed *E. coli* YidC variants. The *numbers* in *parentheses* indicate the positions of amino acid residues in *E. coli* YidC, and the deletion fragments are colored as in *A*. The prolines in TM2 are indicated by a *circled P*. Because of the structural disorder of cytosolic loop C2 and the C terminus in *E. coli* YidC, the YidCΔ6, YidCΔ7, and YidCΔC variants are not shown in *A*. In addition, a summary of the growth complementation by the variants is indicated for FTL10 cells grown under aerobic and anaerobic conditions as described under "Experimental Procedures" and in the legend of Fig. 2.

sion times for the two-component analysis were determined in separate experiments. The diffusion of YidC-Nd alone was taken from measurements in the absence of RNC-F_{0C}, and the YidC-Nd·RNC-F_{0C} complex was approximated by measurements with labeled RNC-F_{0C} alone. During fitting, the two diffusion times were fixed, and only the amplitudes were varied. The fluorescence lifetime data available within our FCS data indicate that binding of RNC-F_0C does not alter the fluorescence intensity. Hence, the amplitude of the two components represents their relative populations. The background fluorescence was analyzed using nonlabeled YidC-Nd and RNCs at stated concentrations. The intensity of the background fluorescence did not exceed 5% of the fluorescently labeled YidC-Nd.

In Vitro Synthesis, Insertion, and Translocation Assay—*In vitro* synthesis of the insertion substrates was performed as described before (30). The *in vitro* transcription and translation was carried out at 37 °C for 20 min in the presence of EasyTag EXPRESS^{35}S protein labeling mix (PerkinElmer Life Sciences) and empty liposomes or proteoliposomes containing YidC and/or SecYEG. A small fraction of the reaction was taken as a synthesis control.

Results

YidC Variants Complement the Growth Defect of a YidC Depletion Strain—To study the role of the cytoplasmic loops in the YidC function, we introduced sequential deletions within YidC as illustrated schematically in Fig. 1. Five deletions of 10 amino acids each were introduced within loop C1 starting at position 374. For loop C2 two deletions, 5 residues each, were introduced starting at position 485. To probe the activity of

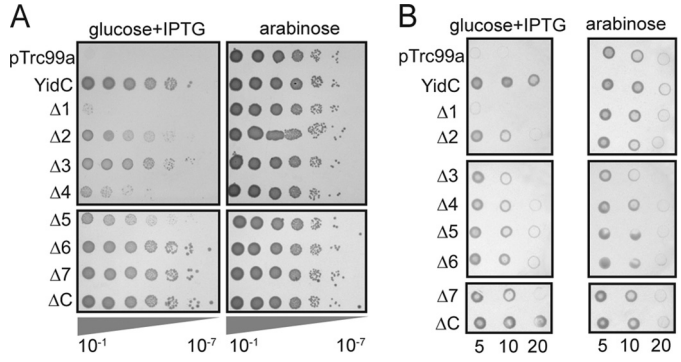

FIGURE 2. **An *in vivo* activity analysis of *E. coli* YidC variants.** *A* and *B*, growth complementation under aerobic (*A*) and anaerobic (*B*) conditions. In the presence of arabinose, all the cells exhibited similar growth phenotype (*right panels*). However, under the condition of glucose repression, differences of cell viability were manifested by a dilution series (*left panels*). pTrc99a, cells containing the empty vector pTrc99a (negative control); *YidC*, cells containing wild-type YidC (positive control); *YidCΔ1–ΔC*, cells containing the YidC variants.

designed YidC variants *in vivo*, pTrc99a plasmids bearing the genes encoding for the YidC mutants were transformed into *E. coli* strain FTL10 (28), in which the endogenous chromosomal *yidC* gene was deleted, whereas a copy of the *yidC* gene was placed under the control of the arabinose-inducible promoter and integrated into the chromosome. Therefore, growth of the FTL10 is strictly arabinose-dependent. In the presence of arabinose, the transcription of the *yidC* gene is initiated, thereby exhibiting normal growth phenotype, whereas glucose supplementation inhibits the chromosomal *yidC* expression. The activity of designed YidC mutants can be examined by observing whether they rescue the growth defect of strain FTL10 when grown with glucose. Cells harboring the YidC variants displayed a robust growth phenotype under arabinose conditions (Fig. 2). However, under glucose and IPTG conditions, different growth phenotypes were observed. As expected, cells containing the empty vector pTrc99a were unable to grow without arabinose, confirming that depletion of native YidC led to the loss of cell viability (4), whereas IPTG-inducible wild-type YidC could compensate for the growth loss (Fig. 2, *YidC*). Remarkably, except for YidCΔ1 (Δ374–383, the numbers represent the position of the amino acid residues in YidC), which failed in growth complementation, all YidC mutants were capable of restoring the growth deficiency of the YidC depletion strain, although to varying extents (Fig. 2*A*, *YidCΔ1–YidCΔ7*). The deletions within the C1 loop had detrimental (YidCΔ1) or moderate (YidCΔ2-Δ5) effects on cell survival, suggesting an important role of the dynamic helical hairpin region for YidC activity (40, 41). Interestingly, a deletion at the tip of the hairpin had the least effect on cell growth (YidCΔ3), because it is unlikely to distort the hairpin structure. Both deletions within loop C2, YidCΔ6 (residues 485–489) and YidCΔ7 (residues 489–493), could fully rescue the growth defect of the YidC defective strain, confirming that the C2 domain of YidC is not crucial for its activity (42). This was also the case for the deletion of the C-terminal end of YidC (YidCΔC) (Δ536–547) in agreement with previous data (24).

Depletion of YidC also impairs cell growth under anaerobic conditions cause by defects in the membrane biogenesis of the anaerobic respiratory complexes, such as NADH dehydrogenase and the F_1F_0 ATPase (43). To determine whether the designed YidC variants could fulfill the growth complementation function under anaerobic conditions, *E. coli* strain FTL10 harboring the genes encoding for YidC variants were grown in anaerobic medium supplemented with 0.5% w/v glycerol and 10 mM sodium fumarate serving as the nonfermentable carbon source and electron acceptor, respectively. As shown in Fig. 2*B*, under arabinose-inducible conditions, the chromosomal copy of *yidC* genes in all strains were fully expressed to maintain growth. Similar to the growth pattern under aerobic conditions, in the presence of IPTG and glucose all the YidC variants, excluding YidCΔ1, were complementation positive and could support cell growth comparable with the wild-type YidC, indicating a generic phenotype of the mutants.

To rule out the possibility that the lack of activity of the YidCΔ1 mutant resulted from poor expression or structural instability, the total membrane fraction containing overexpressed YidCΔ1 protein was isolated and subjected to immunoblotting analysis using antiserum against the polyhistidine tag, wild-type YidC serving as the loading control. Immunoblotting confirmed that the YidCΔ1 variant was expressed at the same level as the wild-type YidC protein (data not shown). Taken together, our data verified that the C2 domain and the C terminus are dispensable for YidC activity, whereas the C1 domain (region 374–383) of YidC is a functionally critical region.

Membrane Insertion of F_0c Is Not Affected by Deletions in YidC Cytoplasmic Loops—As described above, the YidCΔ1 mutant could not restore the growth of the YidC depletion strain. A recent study has also suggested that deletions within the C1 loop dramatically reduced the insertion of YidC-only substrates of Pf3 coat and M13 procoat but had a weak effect on insertion of *E. coli* endogenous protein CyoA (41). Here, we set out to test whether truncated variants of YidC could still fulfill the role as insertases in the *in vitro* membrane insertion of an endogenous substrate. F_0c is a small membrane-embedded subunit c of F_1F_0 ATPase that exclusively relies on YidC for the membrane insertion (Fig. 3*A*) (7, 45). To test the YidC insertion activity, the established *in vitro* co-transcription, translation, and insertion assay in the presence of [^{35}S]methionine and YidC-containing proteoliposomes was employed. Purified YidC variants were reconstituted into liposomes composed of *E. coli* phospholipids. SDS-PAGE demonstrated that all variants could be reconstituted into the liposomes as efficient as the wild-type YidC (Fig. 3, *B* and *D*). Subsequently, the lipid bilayer insertion efficiency of newly synthesized F_0c was assessed by the protein accessibility to proteinase K.

As expected, there was no insertion in the absence of proteoliposomes, and the synthesized F_0c was fully digested by proteinase K (Fig. 3*C*, *buffer lane*). Despite the background insertion resulting from the empty liposomes, a significant protease-protected fraction of F_0c was observed when wild-type YidC-containing proteoliposomes were present (Fig. 3*C*, *lane WT*). Remarkably, protease K-resistant F_0c was also observed when YidCΔ1-containing proteoliposomes were introduced in the *in vitro* transcription/translation system (Fig. 3*C*, *lane Δ1*). Also, all other designed YidC mutants demonstrated insertase

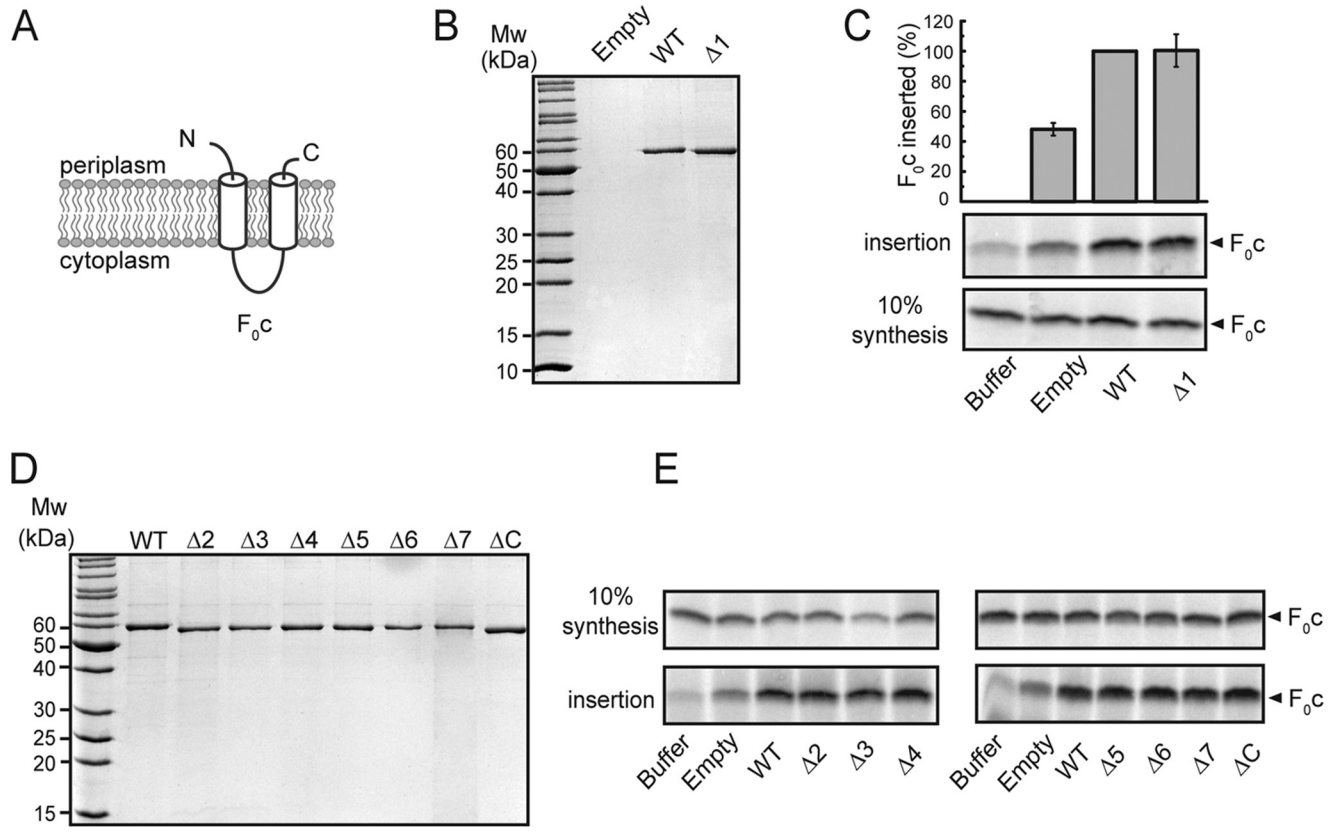

FIGURE 3. **The effect of cytoplasmic loops deletions in YidC on the membrane insertion of F_0c.** *A*, a topology diagram of *E. coli* endogenous substrates F_0c. *B* and *D*, the YidC variant proteins was reconstituted into the *E. coli* liposomes and monitored by 12.5% SDS-PAGE, with empty liposomes (*Empty*) and proteoliposomes-reconstituted WT YidC as negative and positive controls, respectively. *C* and *E*, the *in vitro* synthesis and insertion of F_0c were carried out as described under "Experimental Procedures." After conducting the synthesis/insertion at 37 °C for 20 min, 10% of the reaction volume was taken as a synthesis control, and the rest was subjected to proteinase K treatment and TCA precipitation. *Buffer*, buffer without liposomes; *Empty*, empty liposomes; *WT*, wild-type YidC-containing proteoliposomes; *YidCΔ1–ΔC*, YidC variants-containing proteoliposomes; *Mw*, molecular mass markers.

activity of the F_0c substrate at a level similar to the wild-type YidC (Fig. 3*E*). Our data suggest that the region 374–383 of YidC is not essential for insertion activity despite its disabled function in cell growth complementation. In addition, no other specific region within the cytosolic domains of YidC was solely found to be responsible for the insertase activity.

Cytosolic Loop C2 and the C Terminus of YidC Determine Interactions with Ribosomes—To probe the interaction of YidC with programmed ribosomes, we employed the highly sensitive confocal microscopy-based technique of FCS (46). In FCS, fluorescence fluctuations arising from labeled molecules migrating through the confocal volume of a laser beam are recorded and autocorrelated over the recording time. For the case of translational diffusion, the average residence time of the molecule within the illuminated confocal volume can be measured by FCS, and it is inversely proportional to the diffusion coefficient *D*, which is determined by the hydrodynamic radius of the molecule. Thus, interactions of a small membrane protein, such as YidC, with a large macromolecular complex, such as the ribosome, can be unambiguously detected because of a decrease in the protein's diffusion coefficient.

To exclude the unspecific binding of YidC to ribosomes, the measurements were performed with Alexa Fluor 488-labeled YidC reconstituted into a lipid membrane provided by nanodiscs (24) (Fig. 4). Autocorrelation curves were fitted using the two-component model as described previously (24, 34). As suggested by the autocorrelation function of nanodisc-embedded YidC, diffusion coefficients for all YidC variants varied within a narrow range of 39 ± 2 cm^2/s. To monitor the binding of YidC to ribosomes, RNC-F_0c complexes (Fig. 4) were added in 5-fold excess to YidC-Nd, and the binding efficiency was analyzed based on the shift of the autocorrelation curves caused by the change in the size-dependent diffusion coefficient (Fig. 5*A*). Interactions of wild-type YidC-Nd with RNCs caused a prominent shift in the autocorrelation trace, whereas only weak binding accounting for ~20% of nanodiscs was observed for the C-terminal truncated YidC at the same ribosome:YidC ratio (Fig. 5*A*) in agreement with previously published data (24).

RNC binding was analyzed for all YidC variants, and their binding efficiencies were calculated. Deletions within the C1 domain of YidC had no influence on the ribosome binding efficiency (Fig. 5*B*), and the YidCΔ1 variant, which severely compromised YidC functionality in the cell viability assay (Fig. 2), exhibited full binding efficiency to RNCs (Fig. 5*C*). In contrast, deletion of the region 485–489 within the C2 domain (YidCΔ6) caused a strong reduction in YidC·ribosome complexes. Only 20% of YidCΔ6 were associated with ribosomes that was similar to YidCΔC variant. The deleted region included a conserved residue, Asp-488, which was previously suggested as a potential "hot spot" in ribosome binding (27). Another truncation within the C2 loop, YidCΔ7, had a weaker effect on RNC binding, but it required prolonged incubation up to 20 min to achieve an

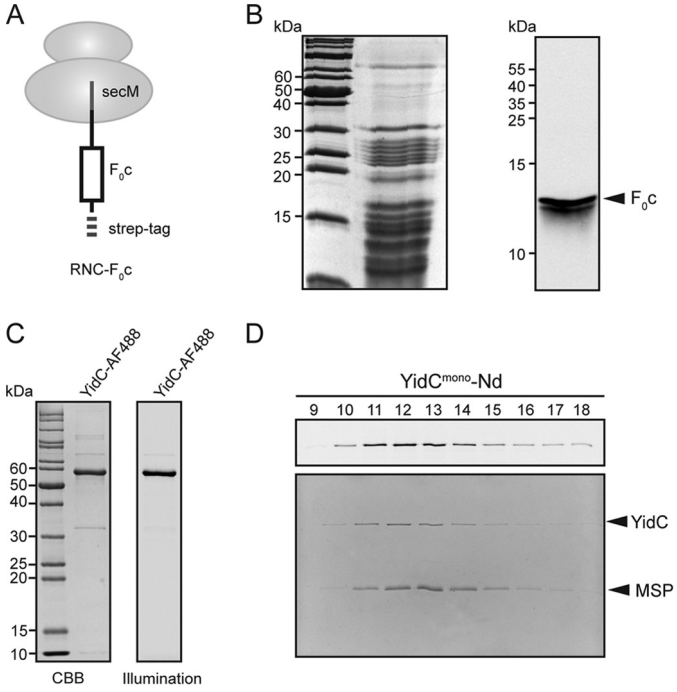

FIGURE 4. **Purification of stalled ribosomes and nanodisc-embedded YidC.** *A*, a schematic representation of the SecM-stalled RNC-F_0c. The stalled polypeptide chain emerging from the ribosome exit tunnel is composed of the first TMS of F_0c with SecM arresting sequence and the triple Strep tag fused to the C and N termini, respectively. *B*, purified RNC-F_0c complexes were visualized on an SDS-PAGE with Coomassie staining (*left panel*), of which the multiple unspecific bands correspond to ribosomal proteins. The stalled F_0c nascent chains in the RNC-F_0c complexes were verified by Western blot using antibody against the Strep tag (*right panel*). *C*, YidC was efficiently conjugated to Alexa Fluor 488-C_5-maleimide at position 269 within the periplasmic loop 1 and analyzed via Coomassie Brilliant Blue (*CBB*) staining (*left panel*) and via fluorescence when illuminated at 488 nm (*right panel*). *D*, YidC was reconstituted into the synthetic lipids with a composition of 30% mol DOPG, 30% mol DOPE, and 40% mol DOPC as described before (24). The YidC-containing nanodiscs were fractionated and separated via size exclusion chromatography (*top panel*, Alexa Fluor 488 fluorescence; *bottom panel*, Coomassie staining). Fraction #13 or #14 was used for ribosome binding analysis.

equilibrium between the free and RNC-bound states. No temporal variations in complex assembly were observed for other YidC variants. This suggests that the modification within the C2 loop altered the binding kinetics, either reducing the association rate or allowing rapid dissociation of the ribosome prior the nascent chain insertion, hence the slow overall binding. The nascent chain exposed contains the first transmembrane domain of F_0 subunit c and a polar purification Strep tag, which needs to be translocated upon the TM insertion, thus posing a potential bottleneck for the insertion process. To test the hypothesis that the tag weakens the binding, we employed RNC-F_0c with a cleavable purification tag of polar N-terminal amino acids that could be specifically cleaved by 3C protease. When the purification tag was removed from the F_0c nascent chain, rapid YidCΔ6:RNC assembly at wild-type levels was observed, whereas binding of other YidC variants was not affected (Fig. 5*C*) as compared with the tagged RNC-F_0c binding (Fig. 5*B*). With the YidCΔC, weak RNC-F_0c binding is observed. To test whether this was mediated by YidC or by hydrophobic interactions between nanodiscs and the transmembrane domain of F_0c, we analyzed interactions between RNC-F_0c and empty nanodiscs containing fluorophore-conjugated lipids. Only 7% of empty nanodiscs were observed in complex with RNCs (Fig. 5, *B* and *C*), suggesting that the truncated variant YidCΔC demonstrated residual affinity to programmed ribosomes. Thus, we conclude that deletions within the C2 loop destabilize the YidC·ribosome complex.

The Cytoplasmic Loop C2 and the C Terminus of YidC Support Insertion Activity—To further investigate the assembly of YidC·RNC complexes, a double truncated YidC variant (YidCΔ8) was cloned and expressed in which both the region 485–489 of C2 and the C terminus were removed (Figs. 6*A* and 5, *D* and *E*). The nanodisc-reconstituted YidCΔ8 variant demonstrated a weakened interaction with RNC-F_0c, although the interaction appeared to be higher than for the YidCΔC variant (Fig. 5*C*). YidCΔ8 was further subjected to activity tests via the growth complementation and F_0c membrane insertion assays. Although no effect was observed for the individual deletions YidCΔ6 and YidCΔC (Fig. 1), the combination of these truncations within YidC only weakly suppressed the growth deficiency of the YidC depletion strain both under aerobic (Fig. 6*B*) and anaerobic conditions (data not shown). To analyze the membrane insertion of F_0c, YidCΔ8-containing proteoliposomes were introduced into the *in vitro* transcription/translation reaction system, and insertion was tested. Remarkably, the double deletion in YidC had a detrimental impact on its insertion activity *in vitro*. Upon removal of the region 485–489 and the C terminus, YidC was not capable of stimulating the membrane insertion of F_0c (Fig. 6*C*), whereas single truncated YidC variants were fully functional in the assay.

To further verify the inhibitory effect of mutations on the YidC activity, membrane insertion of another YidC exclusive substrate MscL was explored. Similarly to F_0c, MscL is a double-spanning membrane protein (Fig. 6*D*), but with both the N terminus and the long C terminus protruding into the cytoplasmic environment and requiring SRP for membrane targeting and insertion (9, 47). After treatment with proteinase K, the C-terminal region of membrane-inserted MscL was largely digested. The amount of the truncated N-terminal fragment MscL(ΔC) was visualized by phosphor imaging and quantified to assess the insertion efficiency (Fig. 6, *D* and *E*). The wild-type YidC and the YidCΔ1 variant bearing the N-terminal deletion within the C1 loop were equally functional with respect to MscL insertion, suggesting that the protein is capable of interacting with SRP. In contrast, YidCΔ8 was totally inactive in stimulating the membrane insertion of MscL, whereas full activity was observed for the individual deletions YidCΔ6 and YidCΔC (Fig. 6, *D* and *E*). The data suggest that loop C2 together with the C terminus are essential for stabilizing the functional interaction of YidC with translating ribosomes, thereby allowing for the membrane insertion, and these domains may cooperate in maintaining the YidC activity. It is likely that the double deletion within YidC perturbed its structure, which stimulated recruitment of ribosomes as observed in FCS experiments without forming a functional YidC·RNC complex.

The Cytoplasmic Loop C2 and the C Terminus of YidC Are Required for Efficient Membrane Insertion of NuoK—In *E. coli*, YidC functions either independently or in cooperation with SecYEG translocon. In the SecYEG-mediated co-translational

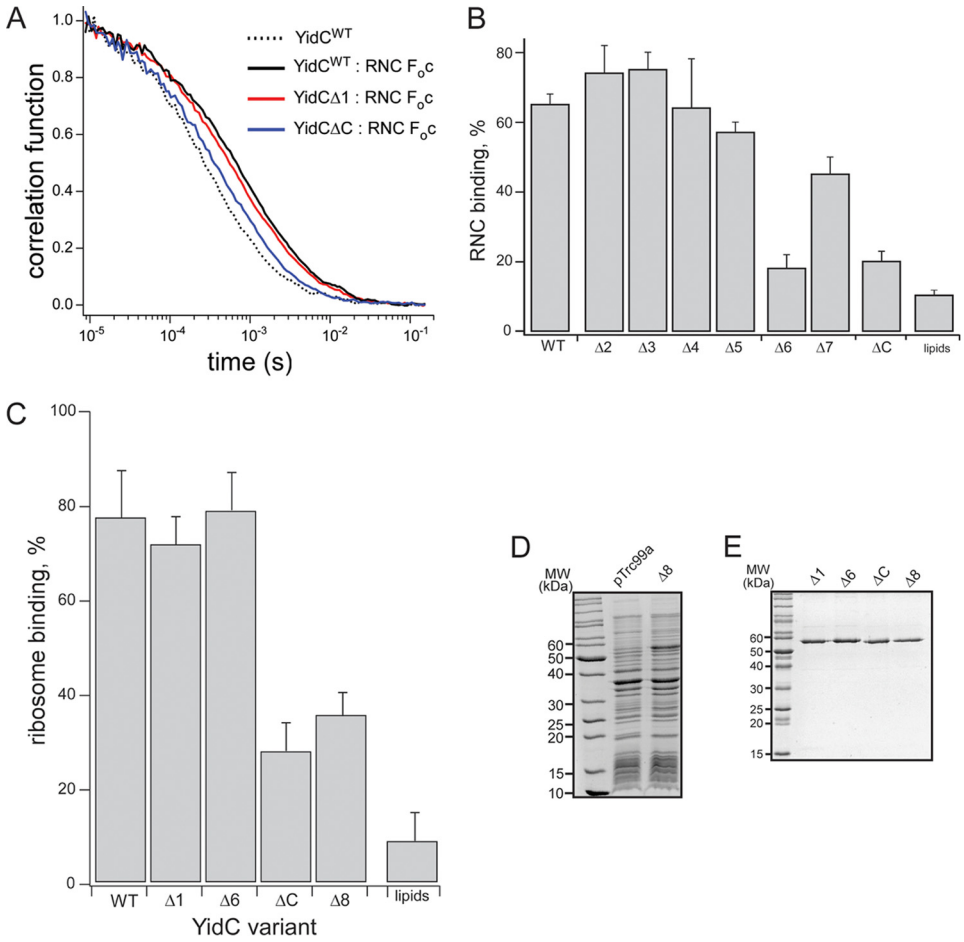

FIGURE 5. **FCS analysis of the YidC·RNC interaction.** *A*, FCS of the interaction between YidC mutants and RNCs. Autocorrelation functions determined from FCS measurements of nanodisc-embedded YidC freely diffusing in solution in the absence and presence of RNCs. Binding of designed YidC variants to the ribosome dramatically reduced their diffusional mobility of YidC-Nd, manifested by a shift of the autocorrelation curve. *B*, the populations of free and ribosome-bound YidC-Nd estimated from the quantitative analysis of the autocorrelation functions for all YidC variants using a two-component model. *C*, YidC-Nd binding to RNC-F_0c in the absence of the purification tag. Upon adding 100 nM tag-less RNCs to YidC-Nd, binding of YidC was analyzed by means of FCS. Removal of the hydrophilic purification tag at the F_0c nascent chain recovered binding of YidCΔ6 to programmed ribosomes. However, the interaction of YidCΔC remained weak but above the background unspecific binding of the nascent chain to the nanodiscs. *D*, YidCΔ8 was efficiently reconstituted into *E. coli* liposomes. Expression of the YidCΔ8 variant was visible on SDS-PAGE. *E*, isolated YidCΔ8 was reconstituted into *E. coli* proteoliposomes similar to the other YidC variants. *pTrc99a*, empty vector.

pathway, YidC is suggested to localize in the vicinity of the lateral gate of SecY to facilitate the release of the TMSs from the SecYEG channel into the lipids bilayers and to chaperone the folding and/or assembly (44, 48). To further examine whether YidCΔ8 is still functional in the SecYEG-YidC insertion pathway, the membrane insertion of NuoK was explored. NuoK is a small membrane subunit K of the NADH dehydrogenase (Fig. 7*A*), requiring both SecYEG and YidC for efficient membrane insertion (13). To study the *in vitro* membrane insertion of NuoK, YidC together with SecYEG were integrated into liposomes to obtain SecYEG-YidC-containing proteoliposomes (Fig. 7*B*). Subsequently, YidC-SecYEG proteoliposomes were introduced into the NuoK synthesis system, and the amount of proteinase-protected NuoK fragments (13) was analyzed and quantified as described (Fig. 7*C*). A decrease in the amount of membrane-inserted NuoK was observed for the YidCΔ8 mutant, down to ~70% of the wild-type YidC. With YidCΔ1 and YidCΔ6, full functionality was retained with respect to the membrane insertion of NuoK. This suggests that the cytosolic loop 2 and the C terminus are needed for the efficient insertion of NuoK that is YidC- and Sec-dependent.

Discussion

Despite recent structural insights, the exact molecular mechanisms of YidC-mediated membrane protein biogenesis remain unknown. YidC has been described to participate in a range of cellular reactions, including ribosome and SRP binding, Sec translocon interactions, and insertion, folding, and oligomerization of its substrates (1). Hence, a comprehensive methodological approach is required to address particular aspects of the insertase functionality. Previous studies using the C-terminal deletion suggested that this domain is involved in ribosome binding (24), as has also been shown for the YidC homologues in Gram-positive and Gram-negative bacteria (24–26). However, with the *E. coli* YidC, a substantial residual binding of translating ribosomes was observed, and the truncated YidC variant was fully active in insertion and could rescue growth of YidC-depleted cells. Thus, the C terminus of *E. coli* YidC was

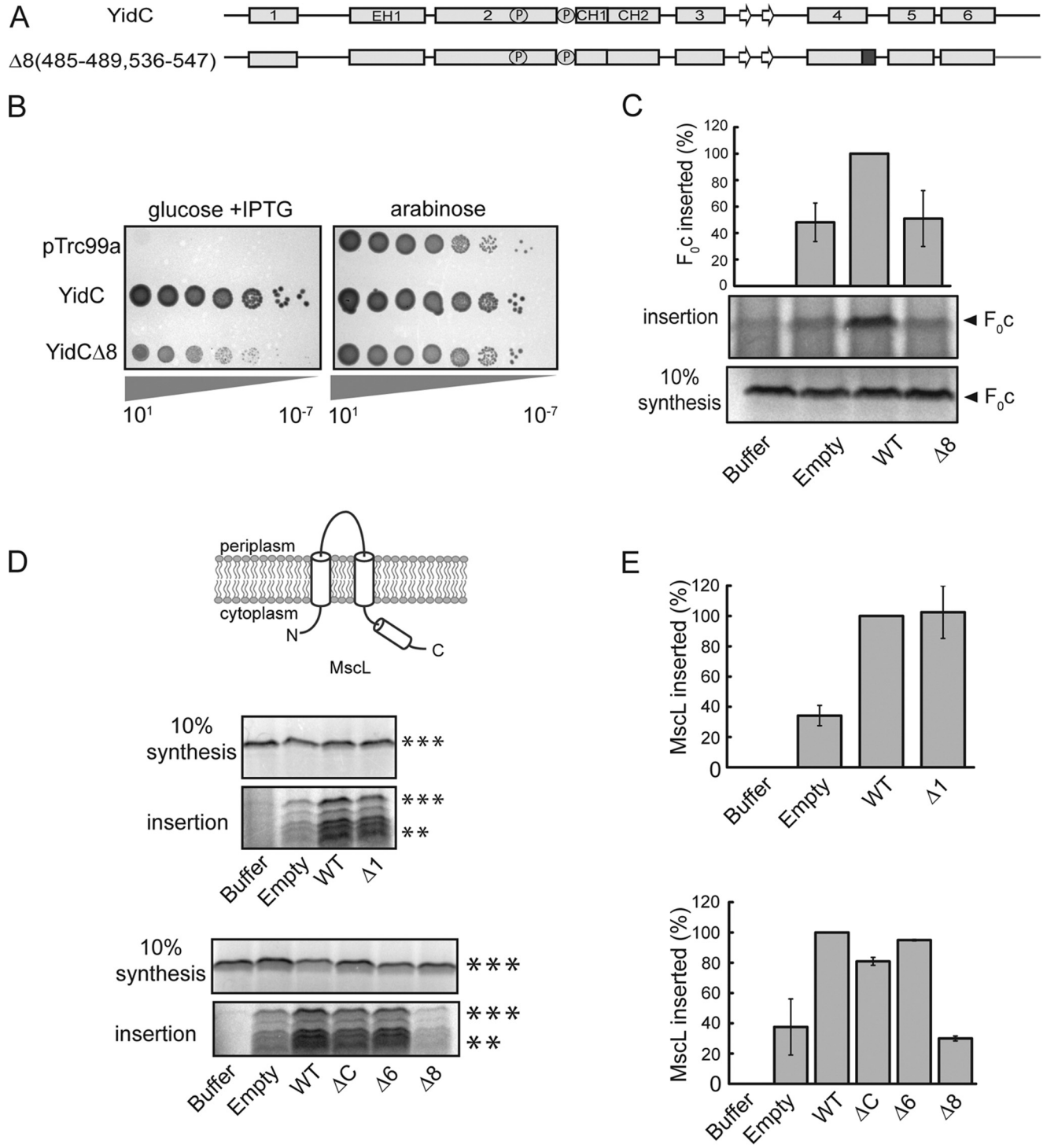

FIGURE 6. **The effect of deletion of the C terminus and C2(485–489) region of YidC on the insertion of F_0c and MscL.** *A*, a schematic representative of the YidC double deletions mutant (YidCΔ8). The region 485–489 of the C2 domain and the C terminus of YidC were removed. *B*, results from growth complementation test suggest limited functionality of YidCΔ8 *in vivo*. *C–E*, membrane insertion of YidC-dependent substrates F_0c (*C*) and MscL (*D* and *E*) were assayed and quantified. ***, full-length MscL; **, proteinase K-resistant bands. To quantify the insertion efficiency, the amount of F_0c and MscL inserted by wild-type YidC was set to 100, and the insertion mediated by YidC variants was normalized to this value. *Empty*, empty liposomes; *WT*, wild-type YidC-containing proteoliposomes; *Δ6*, YidCΔ6-containing proteoliposomes; *ΔC*, YidCΔC-containing proteoliposomes; *Δ8*, YidCΔ8-containing proteoliposomes. The data shown were derived from three independent experiments, and calculated standard deviation intervals are shown.

thought not to be the only determinant for communication with the ribosome, and the positively charged cytosolic loops were suggested as potential binding partners (24, 27). In this study, we applied both *in vivo* and *in vitro* analyses to investigate the roles played by the cytosolic domains of *E. coli* YidC in its functioning. We could demonstrate that the cytosolic loop C2 and the C-terminal end of YidC determine ribosome binding and the insertion activity, whereas the C1 loop is essential for cell viability and may be involved in downstream protein biogenesis.

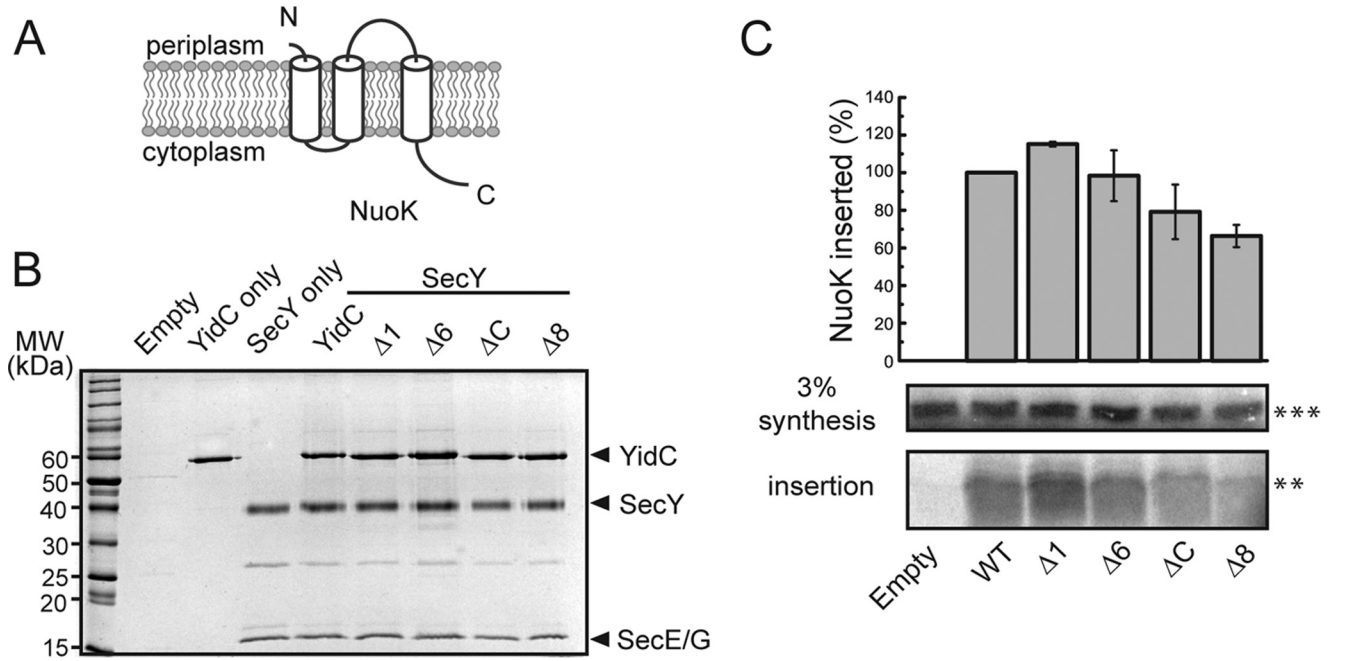

FIGURE 7. **Double deletions interfere with YidC functioning in the membrane insertion of NuoK.** *A*, a topology diagram of *E. coli* endogenous substrates NuoK. *B*, protein profiles of co-reconstituted YidC and SecYEG into *E. coli* liposomes. YidC and SecYEG were co-reconstituted at the molar ratio of 1:1. *C*, NuoK insertion was analyzed via the proteinase K protection assay. After *in vitro* synthesis and proteinase K digestion, the membrane-inserted amount of the proteinase K-resistant bands corresponding to the C-terminal deleted version (**) stimulated by both YidC and SecYEG were probed on 16% Tricine gel. 3% of the synthesis reaction was loaded as a control. Protease-protected NuoK and derived fragments were quantified. The amount of inserted NuoK in the presence of wild-type YidC was set to 100. All the data points shown are obtained from the average of three independent experiments, and calculated standard deviation intervals are shown.

Crystal structures of YidC proteins from *B. halodurans* and *E. coli* (20, 40), as well as co-evolution based modeling (27), demonstrate that the large cytosolic loop C1 is folded into a helical hairpin that protrudes from the membrane plane with a tilt determined by an N-terminal proline residue (position 371 within *E. coli* YidC). Point mutations Y370A and Y377A at the N-terminal end of the loop inactivate YidC *in vivo* (27), whereas mutations, but not deletions, within the hairpin did not interfere with YidC functionality. This domain forms a potential interface for ribosome binding. Previous studies provided conflicting views on its role. Deletion of the entire C1 domain (positions 371–416) inactivated YidC for growth complementation and membrane insertion of Pf3 and M13 procoat proteins (41), whereas in another study, the C1 region was found to be dispensable for YidC activity (42). We observed that the YidCΔ1 mutant bearing an N-terminal deletion of the helical hairpin was severely compromised in growth complementation both under aerobic and anaerobic conditions. Because YidCΔ1 was steadily expressed, the phenotype was not caused by the *in vivo* instabilities and suggested an essential role of the region 374–383 within the C1 domain of YidC in cell viability, in accordance with the recent data (27). However, neither ribosome binding nor membrane protein insertion was affected, as tested *in vitro* for the YidC-only and the SecYEG-associated pathways. Other deletions within the C1 loop had moderate effects on cell viability but also did not reveal defects in ribosome interactions or membrane insertion of F_0c and MscL. Thus, there is a low correlation between the YidC insertase activity and *in vivo* functionality for this domain. We hypothesize that the C1 region of YidC is involved in the membrane insertion of yet unknown substrates that are essential for cell viability or that it plays an important role in chaperone activities such as correct folding of inserted membrane proteins, substrate oligomerization, or protein-protein interactions at the membrane interface.

The conformation of the C2 loop could not be resolved in crystal structures of YidC, suggesting that it is flexible. The loop is built of ~10 amino acids and contains one conserved charged residue Asp-488. A negatively charged residue is essential in this position for cell viability (27). When introducing short deletions within this loop, we observed fully functional YidC with respect to cell viability and substrate membrane insertion. Although these deletions did not affect the insertase activity of YidC *in vitro*, they inhibited or slowed down the assembly of YidC·RNC complexes. In contrast to the C-terminal deletion, ribosome interactions could be restored either upon prolonged incubation or by increasing the hydrophobicity of the nascent chain. Thus, the loop C2 ensures the stable docking of a translating ribosome to YidC, whereas modifications within this region lead to enhanced ribosome dissociation. Hence, the YidC·ribosome complexes may dissociate before the initiation of the co-translational membrane insertion, leading to termination of the membrane insertion events.

Remarkably, combining deletions within the C2 loop (region 485–489) and at the C terminus of YidC (YidCΔ8) abolished the functionality of YidC in the membrane insertion of the YidC-only substrates F_0c and MscL. It is unlikely that this phenotype arises from the instability of the YidCΔ8 variant because a considerable amount of overexpressed YidCΔ8 could be detected, purified, and reconstituted into the liposomes and

nanodiscs. Moreover, using NuoK as a model substrate, we found that YidCΔ8 was also less efficient in the SecYEG-YidC co-translational insertion pathway. The double deletion of the C2 and C terminus likely induces a conformational alteration of YidC that negatively affects insertion.

In conclusion, our findings provide insights into the associations between the insertion activity of YidC and ribosome binding. We demonstrated that the cytosolic loop C2 together with the C terminus of *E. coli* YidC are critical for the assembly of functional YidC·RNCs complexes at the membrane interface, whereas the loop C1 is involved in other vital functions of YidC.

Acknowledgments—We thank Stephan Wickles for valuable discussions and for providing the pEM36-F_Oc plasmid and Anne-Bart Seinen for helpful discussions and contributions on drawing the structure of the YidC variants.

References

1. Dalbey, R. E., Kuhn, A., Zhu, L., and Kiefer, D. (2014) The membrane insertase YidC. *Biochim. Biophys. Acta* **1843,** 1489–1496
2. Wang, P., and Dalbey, R. E. (2011) Inserting membrane proteins: the YidC/Oxa1/Alb3 machinery in bacteria, mitochondria, and chloroplasts. *Biochim. Biophys. Acta* **1808,** 866–875
3. du Plessis, D. J., Nouwen, N., and Driessen, A. J. (2011) The Sec translocase. *Biochim. Biophys. Acta* **1808,** 851–865
4. Samuelson, J. C., Chen, M., Jiang, F., Möller, I., Wiedmann, M., Kuhn, A., Phillips, G. J., and Dalbey, R. E. (2000) YidC mediates membrane protein insertion in bacteria. *Nature* **406,** 637–641
5. Samuelson, J. C., Jiang, F., Yi, L., Chen, M., de Gier, J. W., Kuhn, A., and Dalbey, R. E. (2001) Function of YidC for the insertion of M13 procoat protein in *Escherichia coli*. *J. Biol. Chem.* **276,** 34847–34852
6. Chen, M., Samuelson, J. C., Jiang, F., Muller, M., Kuhn, A., and Dalbey, R. E. (2002) Direct interaction of YidC with the Sec-independent Pf3 coat protein during its membrane protein insertion. *J. Biol. Chem.* **277,** 7670–7675
7. van der Laan, M., Bechtluft, P., Kol, S., Nouwen, N., and Driessen, A. J. (2004) F_1F_0 ATP synthase subunit c is a substrate of the novel YidC pathway for membrane protein biogenesis. *J. Cell Biol.* **165,** 213–222
8. Neugebauer, S. A., Baulig, A., Kuhn, A., and Facey, S. J. (2012) Membrane protein insertion of variant MscL proteins occurs at YidC and SecYEG of *Escherichia coli*. *J. Mol. Biol.* **417,** 375–386
9. Price, C. E., Kocer, A., Kol, S., van der Berg, J. P., and Driessen, A. J. (2011) *In vitro* synthesis and oligomerization of the mechanosensitive channel of large conductance, MscL, into a functional ion channel. *FEBS Lett.* **585,** 249–254
10. Aschtgen, M. S., Zoued, A., Lloubès, R.,Journet, L., and Cascales, E. (2012) The C-tail anchored TssL subunit, an essential protein of the enteroaggregative *Escherichia coli* Sci-1 Type VI secretion system, is inserted by YidC. *Microbiologyopen* **1,** 71–82
11. van Bloois, E., Haan, G.-J., de Gier, J.-W., Oudega, B., and Luirink, J. (2006) Distinct requirements for translocation of the N-tail and C-tail of the *Escherichia coli* inner membrane protein CyoA. *J. Biol. Chem.* **281,** 10002–10009
12. du Plessis, D. J., Nouwen, N., and Driessen, A. J. (2006) Subunit a of cytochrome *o* oxidase requires both YidC and SecYEG for membrane insertion. *J. Biol. Chem.* **281,** 12248–12252
13. Price, C. E., and Driessen, A. J. (2010) Conserved negative charges in the transmembrane segments of subunit K of the NADH:ubiquinone oxidoreductase determine its dependence on YidC for membrane insertion. *J. Biol. Chem.* **285,** 3575–3581
14. Yi, L., Celebi, N., Chen, M., and Dalbey, R. E. (2004) Sec/SRP requirements and energetics of membrane insertion of subunits a, b, and c of the *Escherichia coli* F_1F_0 ATP Synthase. *J. Biol. Chem.* **279,** 39260–39267
15. Zhu, L., Wasey, A., White, S. H., and Dalbey, R. E. (2013) Charge composition features of model single-span membrane proteins that determine selection of YidC and SecYEG translocase pathways in *Escherichia coli*. *J. Biol. Chem.* **288,** 7704–7716
16. Zhu, L., Kaback, H. R., and Dalbey, R. E. (2013) YidC protein, a molecular chaperone for LacY protein folding via the SecYEG protein machinery. *J. Biol. Chem.* **288,** 28180–28194
17. Wagner, S., Pop, O. I., Pop, O., Haan, G.-J., Baars, L., Koningstein, G., Klepsch, M. M., Genevaux, P., Luirink, J., and de Gier, J.-W. (2008) Biogenesis of MalF and the $MalFGK_2$ maltose transport complex in *Escherichia coli* requires YidC. *J. Biol. Chem.* **283,** 17881–17890
18. Funes, S., Kauff, F., van der Sluis, E. O., Ott, M., and Herrmann, J. M. (2011) Evolution of YidC/Oxa1/Alb3 insertases: three independent gene duplications followed by functional specialization in bacteria, mitochondria and chloroplasts. *Biol. Chem.* **392,** 13–19
19. Sääf, A., Monné, M., de Gier, J. W., and von Heijne, G. (1998) Membrane topology of the 60-kDa Oxa1p homologue from *Escherichia coli*. *J. Biol. Chem.* **273,** 30415–30418
20. Kumazaki, K., Kishimoto, T., Furukawa, A., Mori, H., Tanaka, Y., Dohmae, N., Ishitani, R., Tsukazaki, T., and Nureki, O. (2014) Crystal structure of *Escherichia coli* YidC, a membrane protein chaperone and insertase. *Sci. Rep.* **4,** 7299
21. Szyrach, G., Ott, M., Bonnefoy, N., Neupert, W., and Herrmann, J. M. (2003) Ribosome binding to the Oxa1 complex facilitates co-translational protein insertion in mitochondria. *EMBO J.* **22,** 6448–6457
22. Jia, L., Dienhart, M., Schramp, M., McCauley, M., Hell, K., and Stuart, R. A (2003) Yeast Oxa1 interacts with mitochondrial ribosomes: the importance of the C-terminal region of Oxa1. *EMBO J.* **22,** 6438–6447
23. Wu, Z. C., de Keyzer, J., Berrelkamp-Lahpor, G. A., and Driessen, A. J. (2013) Interaction of *Streptococcus mutans* YidC1 and YidC2 with translating and nontranslating ribosomes. *J. Bacteriol.* **195,** 4545–4551
24. Kedrov, A., Sustarsic, M., de Keyzer, J., Caumanns, J. J., Wu, Z. C., and Driessen, A. J. (2013) Elucidating the native architecture of the YidC: ribosome complex. *J. Mol. Biol.* **425,** 4112–4124
25. Kohler, R., Boehringer, D., Greber, B., Bingel-Erlenmeyer, R., Collinson, I., Schaffitzel, C., and Ban, N. (2009) YidC and Oxa1 form dimeric insertion pores on the translating ribosome. *Mol. Cell* **34,** 344–353
26. Seitl, I., Wickles, S., Beckmann, R., Kuhn, A., and Kiefer, D. (2014) The C-terminal regions of YidC from *Rhodopirellula baltica* and *Oceanicaulis alexandrii* bind to ribosomes and partially substitute for SRP receptor function in *Escherichia coli*. *Mol. Microbiol.* **91,** 408–421
27. Wickles, S., Singharoy, A., Andreani, J., Seemayer, S., Bischoff, L., Berninghausen, O., Soeding, J., Schulten, K., van der Sluis, E. O., and Beckmann, R. (2014) A structural model of the active ribosome-bound membrane protein insertase YidC. *Elife* **3,** e03035
28. Hatzixanthis, K., Palmer, T., and Sargent, F. (2003) A subset of bacterial inner membrane proteins integrated by the twin-arginine translocase. *Mol. Microbiol.* **49,** 1377–1390
29. Baneyx, F., and Georgiou, G. (1990) *In vivo* degradation of secreted fusion proteins by the *Escherichia coli* outer membrane protease OmpT. *J. Bacteriol.* **172,** 491–494
30. van der Laan, M., Houben, E. N., Nouwen, N., Luirink, J., and Driessen, A. J. (2001) Reconstitution of Sec-dependent membrane protein insertion: nascent FtsQ interacts with YidC in a SecYEG-dependent manner. *EMBO Rep.* **2,** 519–523
31. Denisov, I. G., Grinkova, Y. V., Lazarides, A. A., and Sligar, S. G. (2004) Directed self-assembly of monodisperse phospholipid bilayer nanodiscs with controlled size. *J. Am. Chem. Soc.* **126,** 3477–3487
32. Kedrov, A., Kusters, I., Krasnikov, V. V., and Driessen, A. J. (2011) A single copy of SecYEG is sufficient for preprotein translocation. *EMBO J.* **30,** 4387–4397
33. Ritchie, T. K., Grinkova, Y. V., Bayburt, T. H., Denisov, I. G., Zolnerciks, J. K., Atkins, W. M., and Sligar, S. G. (2009) Reconstitution of membrane proteins in phospholipid bilayer nanodiscs. *Methods Enzymol.* **464,** 211–231
34. Wu, Z. C., de Keyzer, J., Kedrov, A., and Driessen, A. J. (2012) Competitive binding of the SecA ATPase and ribosomes to the SecYEG translocon. *J. Biol. Chem.* **287,** 7885–7895
35. Bischoff, L., Berninghausen, O., and Beckmann, R. (2014) Molecular basis

for the ribosome functioning as an L-tryptophan sensor. *Cell Rep.* **9,** 469–475
36. Crevenna, A. H., Naredi-Rainer, N., Schönichen, A., Dzubiella, J., Barber, D. L., Lamb, D. C., and Wedlich-Söldner, R. (2013) Electrostatics control actin filament nucleation and elongation kinetics. *J. Biol. Chem.* **288,** 12102–12113
37. Müller, C. B., Loman, A., Pacheco, V., Koberling, F., Willbold, D., Richtering, W., and Enderlein, J. (2008) Precise measurement of diffusion by multi-color dual-focus fluorescence correlation spectroscopy. *Europhys. Lett.* **83,** 46001
38. de Keyzer, J., van der Does, C., Swaving, J., and Driessen, A. J. (2002) The F286Y mutation of PrlA4 tempers the signal sequence suppressor phenotype by reducing the SecA binding affinity. *FEBS Lett.* **510,** 17–21
39. Hanahan, D. (1983) Studies on transformation of *Escherichia coli* with plasmids. *J. Mol. Biol.* **166,** 557–580
40. Kumazaki, K., Chiba, S., Takemoto, M., Furukawa, A., Nishiyama, K., Sugano, Y., Mori, T., Dohmae, N., Hirata, K., Nakada-Nakura, Y., Maturana, A. D., Tanaka, Y., Mori, H., Sugita, Y., Arisaka, F., Ito, K., Ishitani, R., Tsukazaki, T., and Nureki, O. (2014) Structural basis of Sec-independent membrane protein insertion by YidC. *Nature* **509,** 516–520
41. Chen, Y., Soman, R., Shanmugam, S. K., Kuhn, A., and Dalbey, R. E. (2014) The role of the strictly conserved positively charged residue differs among the Gram-positive, Gram-negative and chloroplast YidC homologs. *J. Biol. Chem.* **289,** 35656–35667
42. Jiang, F., Chen, M., Yi, L., de Gier, J.-W., Kuhn, A., and Dalbey, R. E. (2003) Defining the regions of *Escherichia coli* YidC that contribute to activity. *J. Biol. Chem.* **278,** 48965–48972
43. Price, C. E., Otto, A., Fusetti, F., Becher, D., Hecker, M., and Driessen, A. J. (2010) Differential effect of YidC depletion on the membrane proteome of *Escherichia coli* under aerobic and anaerobic growth conditions. *Proteomics* **10,** 3235–3247
44. Sachelaru, I., Petriman, N. A., Kudva, R., Kuhn, P., Welte, T., Knapp, B., Drepper, F., Warscheid, B., and Koch, H.-G. (2013) YidC occupies the lateral gate of the SecYEG translocon and is sequentially displaced by a nascent membrane protein. *J. Biol. Chem.* **288,** 16295–16307
45. Kol, S., Nouwen, N., and Driessen, A. J. (2008) The charge distribution in the cytoplasmic loop of subunit c of the F_1F_0 ATPase is a determinant for YidC targeting. *J. Biol. Chem.* **283,** 9871–9877
46. Krichevsky, O., and Bonnet, G. (2002) Fluorescence correlation spectroscopy: the technique and its applications. *Reports Prog. Phys.* **65,** 251
47. Pop, O. I., Soprova, Z., Koningstein, G., Scheffers, D.-J., van Ulsen, P., Wickström, D., de Gier, J.-W., and Luirink, J. (2009) YidC is required for the assembly of the MscL homopentameric pore. *FEBS J.* **276,** 4891–4899
48. Ge, Y., Draycheva, A., Bornemann, T., Rodnina, M. V., and Wintermeyer, W. (2014) Lateral opening of the bacterial translocon on ribosome binding and signal peptide insertion. *Nat. Commun.* **5,** 5263